

Nationaal Lucht- en Ruimtevaartlaboratorium

National Aerospace Laboratory NLR



NLR TP 97556

FASTFLO-automatic CFD system for three-dimensional flow simulations

J.W. van der Burg and B. Oskam

DOCUMENT CONTROL SHEET

	ORIGINATOR'S REF. TP 97556 U		SECURITY CLASS. Unclassified		
ORIGINATOR National Aerospace Laboratory NLR, Amsterdam, The Netherlands					
TITLE FASTFLO-automatic CFD system for three-dimensional flow simulations					
PRESENTED AT the Conference on Industrial Technologies and 3rd Aero Days held in Toulouse, France, October, 1997					
AUTHORS J.W. van der Burg and B. Oskam		DATE 971025	pp ref 20 7		
DESCRIPTORS <table style="width: 100%; border: none;"> <tr> <td style="width: 50%; vertical-align: top;"> Aerodynamic configurations Aerodynamic drag Aerodynamic forces Aerodynamics Aircraft configurations Aircraft design Algorithms </td> <td style="width: 50%; vertical-align: top;"> Computational fluid dynamics Computer aided design Computerized simulation Grid generation (mathematics) Navier-stokes equation Numerical analysis Pitching moments </td> </tr> </table>				Aerodynamic configurations Aerodynamic drag Aerodynamic forces Aerodynamics Aircraft configurations Aircraft design Algorithms	Computational fluid dynamics Computer aided design Computerized simulation Grid generation (mathematics) Navier-stokes equation Numerical analysis Pitching moments
Aerodynamic configurations Aerodynamic drag Aerodynamic forces Aerodynamics Aircraft configurations Aircraft design Algorithms	Computational fluid dynamics Computer aided design Computerized simulation Grid generation (mathematics) Navier-stokes equation Numerical analysis Pitching moments				
ABSTRACT <p>In the Brite-Euram project FASTFLO an automatic CFD (Computational Fluid Dynamics) system for three-dimensional flow simulations is developed (Ref. 1). The objectives of this project are defined in terms of</p> <ol style="list-style-type: none"> 1. CFD-problem-turnaround time, and 2. Accuracy of aerodynamic quantities <p>The functionality of the CFD system is defined by its algorithmic components</p> <ul style="list-style-type: none"> • aerodynamic geometry definition, • surface triangulation, • 3D hybrid grid generation (prisms/tetrahedra), • pre-processing, and flow calculation, • grid adaption, • aerodynamic post-processing, and • visualisation. <p>The present paper provides a critical assessment of the automation level and the accuracy of the CFD system under development. Applications will be discussed to demonstrate the capabilities of the FASTFLO CFD system.</p>					

Summary

In the Brite-Euram project FASTFLO¹ an automatic CFD (Computational Fluid Dynamics) system for three-dimensional flow simulations is developed (Ref. 1). The objectives of this project are defined in terms of

1. CFD-problem-turnaround time, and
2. accuracy of aerodynamic quantities

The functionality of the CFD system is defined by its algorithmic components

- aerodynamic geometry definition,
- surface triangulation,
- 3D hybrid grid generation (prisms/tetrahedra),
- pre-processing, and flow calculation,
- grid adaption,
- aerodynamic post-processing, and
- visualisation.

The present paper provides a critical assessment of the automation level and the accuracy of the CFD system under development. Applications will be discussed to demonstrate the capabilities of the FASTFLO CFD system.

¹Partners: NLR, DLR, FFA, SAAB, IBK, DASA-LM



Contents

1	Introduction	5
2	Objectives	6
3	Functionality of the FASTFLO CFD system	7
4	Applications	8
5	Automation level	9
6	Accuracy	11
7	Conclusions	12
8	References	13

1 Introduction

Current forecasts as published by commercial airplane companies foresee a steady growth of air traffic and replacement of aging aircraft over the next 20 years (Refs. 2, 3). To remain competitive on the international airliner market these airplane companies are under pressure to change continuously to more cost efficient development of new aircraft and derivatives. CFD-technology for improved aerodynamic design reducing development costs and allowing faster aircraft development cycles is one of a number of key technologies urgently needed by the European aerospace industry (Ref. 4).

For CFD technology to have an impact on the aerodynamic design of airplanes the first requirement to be satisfied is that the CFD-problem-turnaround-time (incl. grid generation and aerodynamic post-processing) must be of the order of a day to a week, or less. Aerodynamic analysis is a process of looking at a significant number of flow conditions (lift coefficients, Mach numbers, Reynolds numbers) for more than one geometric variant such that a large number of calculations have to be made. If the application of CFD codes does not yield results at this industrial time scale the impact of CFD-technology on aerodynamic design will be reduced (Ref. 5).

A second requirement which needs to be met by CFD tools for the development of commercial transport aircraft is high accuracy of predicted aerodynamic forces such that computed drag, pitching moment and lift can be relied upon to reduce the risks involved in airplane design. This second requirement translates for example into better turbulence models, and extreme grid resolution or automatic, adaptive grid generation if the first requirement (CFD-problem-turnaround-time) is also to be satisfied simultaneously.

2 Objectives

The objective of the FASTFLO project is to develop an automatic CFD system based on the three-dimensional Reynolds-averaged Navier-Stokes equations applicable to complete aircraft configurations e.g. aircraft with engines and high-lift systems. The CFD-system will have to satisfy basic requirements for industrial CFD:

1. CFD-problem-turnaround-time of a day to a week (or less) for very complex geometries.
2. High accuracy of aerodynamic entities (forces, moments and pressures).

The FASTFLO CFD system is based upon the hybrid (prismatic/tetrahedral) grid approach which has the potential to satisfy these two basic requirements on the level of the Reynolds-averaged Navier-Stokes equations. At present the Euler equations are used as a stepping stone towards the Navier-Stokes level.

Technology ready multi-block methods do not satisfy the first requirement (with respect to turnaround time) for complex geometries. The technical limitation of the multi-block method lies in the multi-block grid generation process, which is internationally recognised as a time-consuming process in case of complex geometries despite significant efforts to shorten the turnaround time. For example in the ENIFAIR project a calendar time of one year is planned for the first generation of a viscous multi-block grid for the wing-body-pylon-engine configuration with high-lift devices. Although a second multi-block grid for the same configuration can be generated in a shorter period, a CFD-problem-turnaround time of a week remains a distant achievement for very complex configurations using multi-block methods. In the FASTFLO project this CFD-problem-turnaround time is to be reduced to a week at most by introducing an automated grid generation process.

3 Functionality of the FASTFLO CFD system

An overview of the algorithmic components in the FASTFLO CFD system is shown in Figure 1. Starting point of the FASTFLO CFD system is the master geometry of an aircraft configuration. This master geometry is represented by either multi-block based curves and surfaces or IGES 5.1 curves and surface patches (CAD-format). Important is that the geometric representation of the aerodynamic aircraft configuration is sufficiently continuous, at least C^0 -continuous (airtight) at junction lines.

In the surface triangulation algorithm (see Figure 1) the surfaces of the geometric representation are triangulised. A distribution function in space controls the size of the edges in the surface triangulation. This distribution function is defined by means of source terms and a uniform mesh size. In the 3D hybrid grid generation algorithm a prismatic grid is generated starting from the surface triangulation of the geometric representation. The tetrahedral grid is generated in the remaining part of the flow domain which is bounded by the triangulation of the farfield boundaries, the triangulation of symmetry plane(s) and the outer boundary of the prismatic grid. Subsequently the hybrid grid is formed by connecting the prismatic grid and tetrahedral grid.

A pre-processing algorithm is employed to achieve optimal vector and parallel performance in the flow calculation algorithm on two memory architectures: shared and distributed. In the flow calculation algorithm the three-dimensional Euler and Navier-Stokes equations are discretised based upon the vertex-based approach. Multigrid acceleration is accomplished using an agglomeration algorithm.

One of the advantages of using the hybrid grid approach is that it provides a natural framework for solution-adaptive refinement. Grid adaption is based on local grid refinement using a user-selected adaption indicator.

The post-processing algorithm allows a user to select and calculate aerodynamic quantities which are of interest to him in graphical form. Aerodynamic forces, moments and aerodynamic coefficients (drag and lift) are computed.

In order to improve the workflow using the FASTFLO CFD components, and to present the capabilities as a uniform system to the user, a system integration tool is used to integrate the system.



4 Applications

Four applications are introduced to review the characteristics of the FASTFLO CFD system, see Table 1 and 2. Examples are shown for case 2 in Figure 2, for case 3 in Figure 3 and for case 4 in Figure 4. Starting point for all four cases is a multi-block based surface description of the aircraft configuration. The respective grids (tetrahedral and hybrid) are refined at locations of special interest such as the wing leading edge, wing trailing edge, wing tip and the nose region. The flow solution is obtained by taking a sufficient number of multigrid cycles.

The computing time of the FASTFLO CFD system for these four cases is limited as can be observed in Table 1. The grid dimensions for each case can be found in Table 2. The Euler flow calculations using the classical Jameson scheme are performed on a single processor of the NEC SX4/16. In Table 3 it can be seen that the residuals have converged approximately 3 to 4 orders of magnitude for each case. The grid generation steps are run on a workstation (MIPS R10000). The results demonstrate that the computing time of the CFD system is relatively short; If the parallel version of the Euler flow solver is used the computing time does not seem to be the bottleneck to reach the first objective. The CFD-problem-turnaround-time however also depends on the automation level.

5 Automation level

To achieve the first objective of the FASTFLO project in terms of CFD-problem-turnaround a high automation level of the CFD system is required. From this perspective several critical sections of the FASTFLO CFD algorithms will be pinpointed:

- A An aerodynamic configuration can be defined in any format such as for instance: the sections of a body of a wing, the stereo lithography format, internal-CATIA, IGES, VDAFS, STEP, ICEM-DDN or other CAD data formats. Due to transformation of data from one data-format to another data format critical information can be lost (as experienced in transformations between ICEM-DDN and IGES 5.1). A CAD-specialist needs to repair the geometric surface representation of the aircraft configuration. This critical section of applied CFD activity is kept outside the FASTFLO system, because it belongs to the geometry modelling domain.
- B In the geometric representation of an aircraft configuration based on IGES 5.1 small surface patches may occur due to the inadvertent choice of an excessively large number of surface patches. Such an excessively large number of patches is not needed to represent the master geometry sufficiently accurate. The reduction in the number of surface patches (for instance by concatenating them with other surfaces) can be a time-consuming task.
- C Starting point for the FASTFLO CFD system is considered to be an airtight geometric representation defined in the CAD-format IGES 5.1. Since the master geometry is approximated (by a finite number of curves and surfaces) the definition of C^0 -continuity is relative: C^0 -continuous with respect to some small tolerance. For an aerodynamic configuration defined by 100-200 IGES 5.1 surfaces (which is indicative for the considered CFD applications) the inspection of the C^0 -continuity requirement can require hours to complete.
- D The applied CFD specialist should be able to decide which parts of the aerodynamic configuration should be represented with sufficient grid resolution and which parts should have less grid resolution. This requires that the input geometry of the FASTFLO CFD system should be categorised based on geometrical features, such as for instance the surface curvature. The grid generation algorithms should triangulise the selected geometric parts with sufficient resolution. Currently, the user needs to manually specify source terms to triangulise the relevant parts of the geometric representation of the aerodynamic configuration.
- E Aerodynamic choices concerning flow conditions, flow model, boundary conditions and extent of the flow domain should always be specified by user intervention. Other input-options of the CFD-system should have default values, for example: the number of multigrid levels, the CFL-number, the numerical scheme and other non-essential input options. By providing default values the applied CFD-specialist can reduce the level of uncertainty with respect to

the reliability of the CFD system (i.e. robustness of the grid generation, or robustness of the multigrid convergence acceleration).

- F To be able to detect the detailed features of the three-dimensional flow a grid adaption algorithm based on local grid refinement is adopted. In this algorithm grid adaption indicators are utilised which are a function of user-specified parameters and the calculated flow solution. The grid adaption algorithm should be defined in such a way that desirable flow features are not overlooked, and that non-selected flow features are indeed not resolved.
- G The aerodynamic designer investigates flow calculation results in terms of aerodynamic quantities. Typically these are: the aerodynamic forces, moments acting on part(s) of the aircraft configuration, aerodynamic thrust and drag bookkeeping, force and moment distributions for specified planes, load distributions (spanwise lift and drag), distributions of aerodynamic entities on selected sections. The post-processing algorithm handles the user specification at this point and provides the visual representation of these aerodynamic features. The post-processing algorithm should be organised such that the aerodynamic designer can efficiently define and/or select the aerodynamic quantities of interest to him.

Implementation of algorithmic improvements to eliminate these critical sections would help the aerodynamic designer in reducing the CFD-problem-turnaround time for the aerodynamic configuration under consideration. The items A, B and C propose an improvement of the capabilities of independent CAD systems for geometry modelling.

Items D, E and F can be further automated by the implementation of algorithmic improvements reducing the user interaction to the essential inputs. The automation level that can be achieved for item G will depend on the particular aerodynamic case under consideration. Introduction of templates and/or aerodynamic wizards would be needed to reach a CFD problem-turnaround-time, including aerodynamic post-processing, of one day for very complex aerodynamic cases.

6 Accuracy

For the wing-alone configuration (case 1) a hybrid (prismatic/tetrahedral) grid is generated in the framework of a DLR-NLR cooperation (Ref. 7). In the prismatic part of the grid 25 prism layers are generated in order to accurately capture the boundary layer (wall-normal distance of first grid point is 5.0×10^{-6} based on the wing root chord). The hybrid grid consists of 1.031.683 nodes, 951.930 prismatic elements and 3431.524 tetrahedral elements.

Figures 6 and 5 show the pressure and skin friction distribution at spanwise station $\eta = 0.65$ for the ONERA M6 wing-alone configuration. It can be observed that calculated pressure distribution is close to the wind tunnel result and the numerical result obtained with a technology-ready multi-block structured method.

7 Conclusions

The objectives of the FASTFLO-project are defined in terms of CFD-problem-turnaround time, and accuracy. The present results show that the computing time of the CFD system is relatively short (at Euler level); if the parallel version of the Euler flow solver is used the computing time is not a bottleneck to reach the first objective.

The CFD-problem-turnaround time however also depends on the automation level. Seven critical sections are identified (A through G) that determine the automation level. From the discussion of these critical sections it is concluded that a sufficiently high automation level is within reach.

The accuracy requirement is studied at the level of the Reynolds-averaged Navier Stokes equations in the framework of a DLR-NLR cooperation. The results for a wing-alone configuration demonstrate a good potential for accuracy.

8 References

1. J.W. van der Burg (NLR), B. Oskam (NLR), T. Gerhold (DLR), M. Galle (DLR), T. Berglind (FFA), B. Arlinger (SAAB), G. Kretzschmar (IBK), W. Haase (DASA-LM), "FASTFLO contract no. BRPR-CT96-1084, Annex I Project Programme", NLR CR 96275 L, February 23, 1996.
2. Press release: "Airbus Industry 1997 global market forecast, confirming a very large demand", March, 1997.
3. Press release: "Boeing projects healthy airplane demand over the next twenty years", March, 1997.
4. IMG³: "The aeronautical industries technology needs for the fifth framework programme and beyond", December 12, 1997.
5. P.E. Rubbert, "CFD and the changing world of airplane design", In *ICAS Proceedings, 19th Congress of the International Council of the Aeronautical Sciences*, September, 1994.
6. J.I. van den Berg, H.A. Sytsma and H. Schippers, "Computation of the flow about an F16-like configuration for several flow conditions", NLR TP 95226 U, April 4, 1995.
7. J.E.J. Maseland, "Contributions to the development of turbulent Navier-Stokes flow modelling capabilities using unstructured grids", NLR TR 97390 L, June, 1997

No.	test case	cpu-time grid-gen.	cpu-time flow. calc.	Perc. of an 8 hour working day
1	wing-alone	8m 26s	35 m	9%
2	wing-body	52m 54s	2h 14m	38%
3	wing-body-pylon-nacelle	17 m	13 m	6.3%
4	generic fighter	5 m	8m	3.1 %

Table 1 Computing time for grid generation and Euler flow calculation algorithms for each test case measured in terms of cpu-time and percentage of an 8 hour working day (m=minutes; s=seconds); cpu-time of grid generation measured on workstation (MIPS R10000); cpu-time of flow calculation (including pre-processing) measured on single processor of NEC SX4/16 supercomputer

case	curves	surfaces	nodes aerod. surface	prism layers	nodes prism grid	nodes tetrah. grid
1	31	16	10970	10	120670	194579
2	39	14	65085	-	-	694946
3	88	34	14252	5	85512	61452
4	298	130	11829	-	-	38769

Table 2 Dimensions of the generated tetrahedral and hybrid grid for each test-case

case	$M_{inf ty}$	α	multigrid cycles	orders of convergence
1	0.84	3.06	250	3.1
2	0.8	2.2	300	4.6
3	0.8	2.2	200	2.7
4	0.9	4.12	500	4

Table 3 The flow-conditions, the number of multigrid cycles and the order of convergence of the flow calculation algorithm (using Jameson's scheme) for each test-case

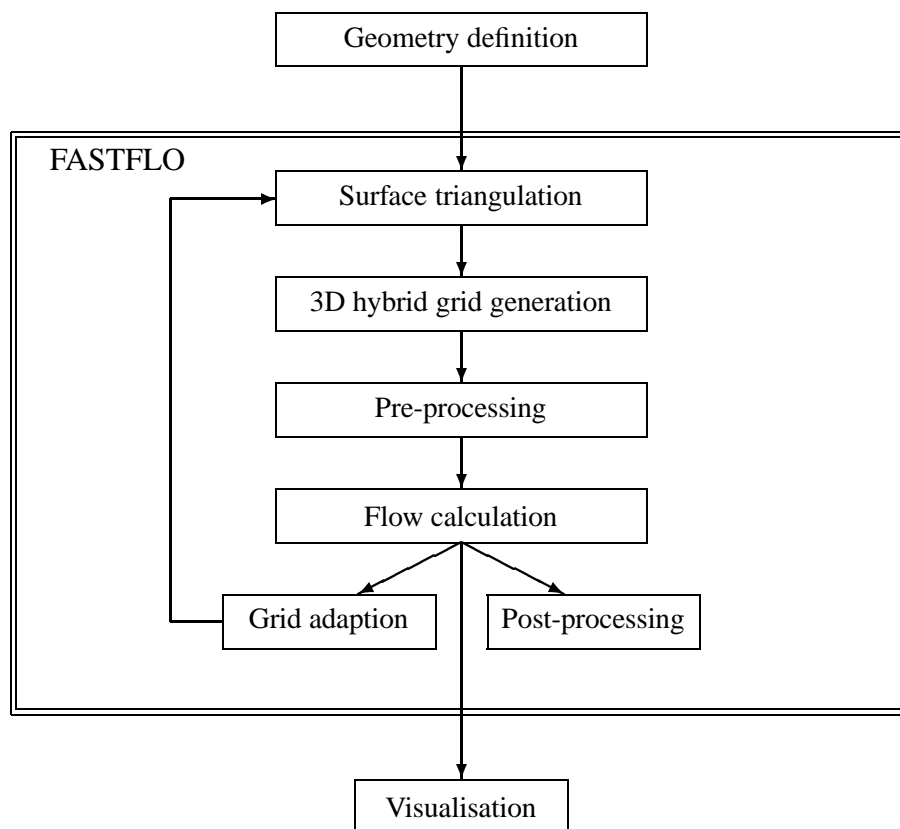


Fig. 1 Algorithmic components of the CFD-system FASTFLO

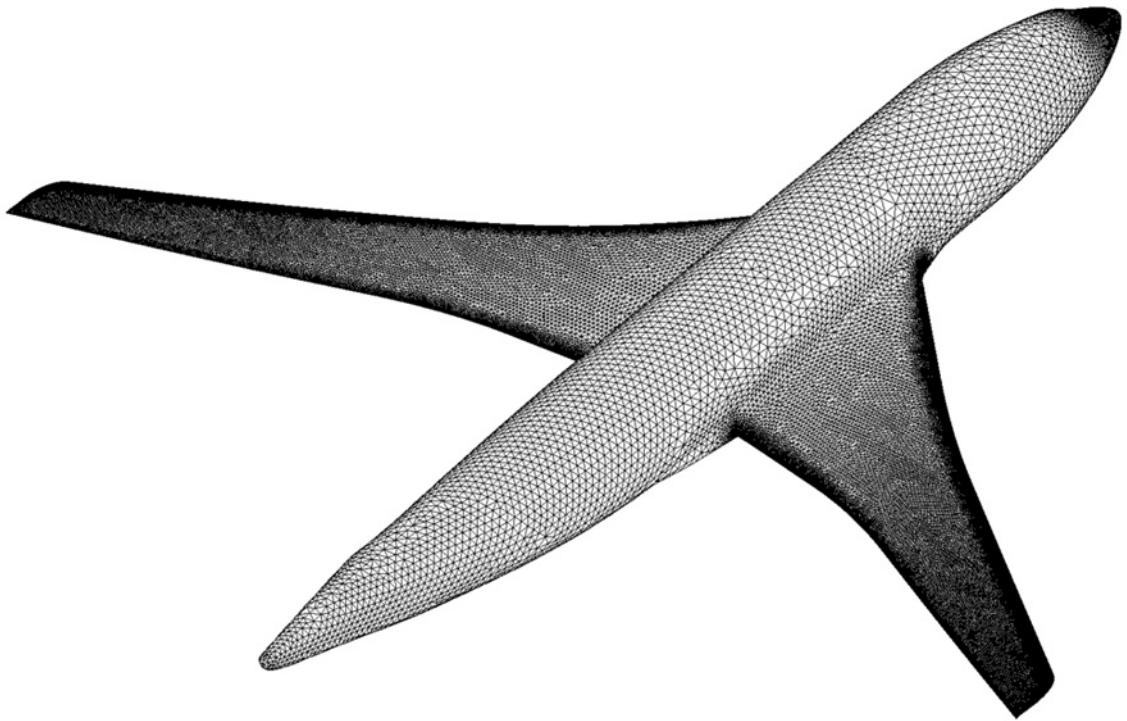


Fig 2 Surface triangulation for the AS28G wing-body configuration

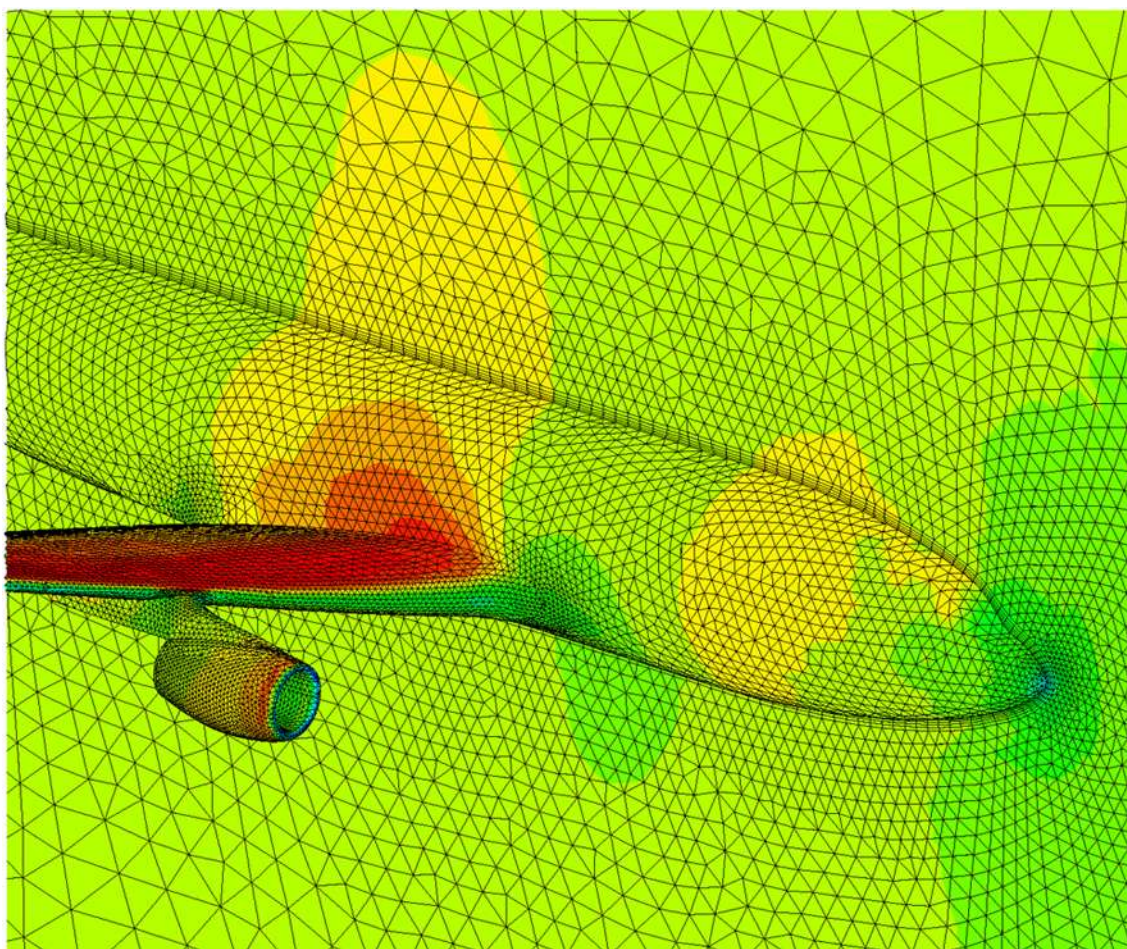


Fig 3 Pressure distribution calculated for the AS28G wing-body-pylon-nacelle configuration on the hybrid (prismatic/tetrahedral) grid; $M_\infty = 0.8$; $\alpha = 2.2$ degrees

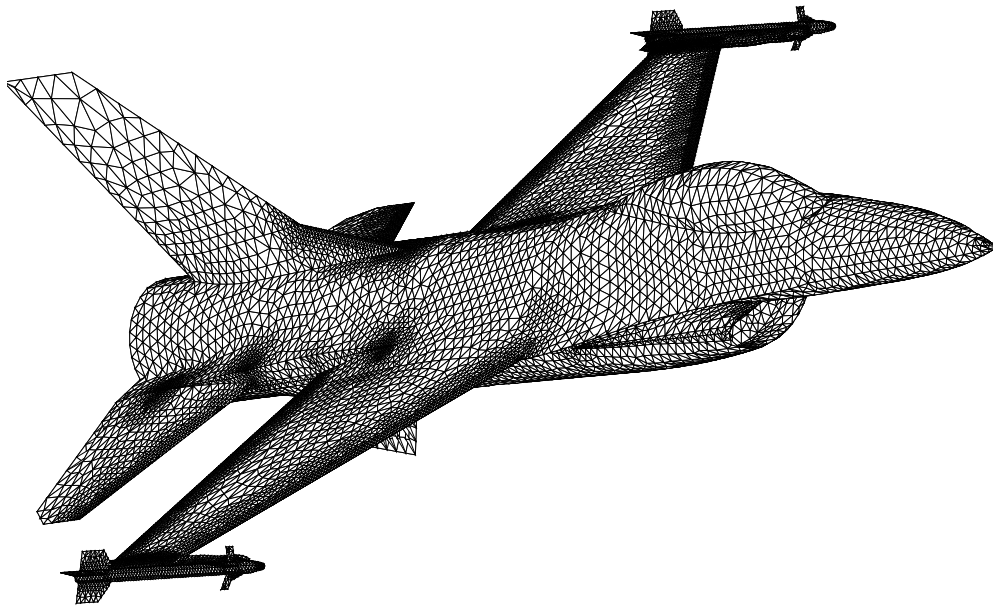


Fig. 4 Surface triangulation for a generic fighter configuration; geometry from J.I. van den Berg (Ref. 6)

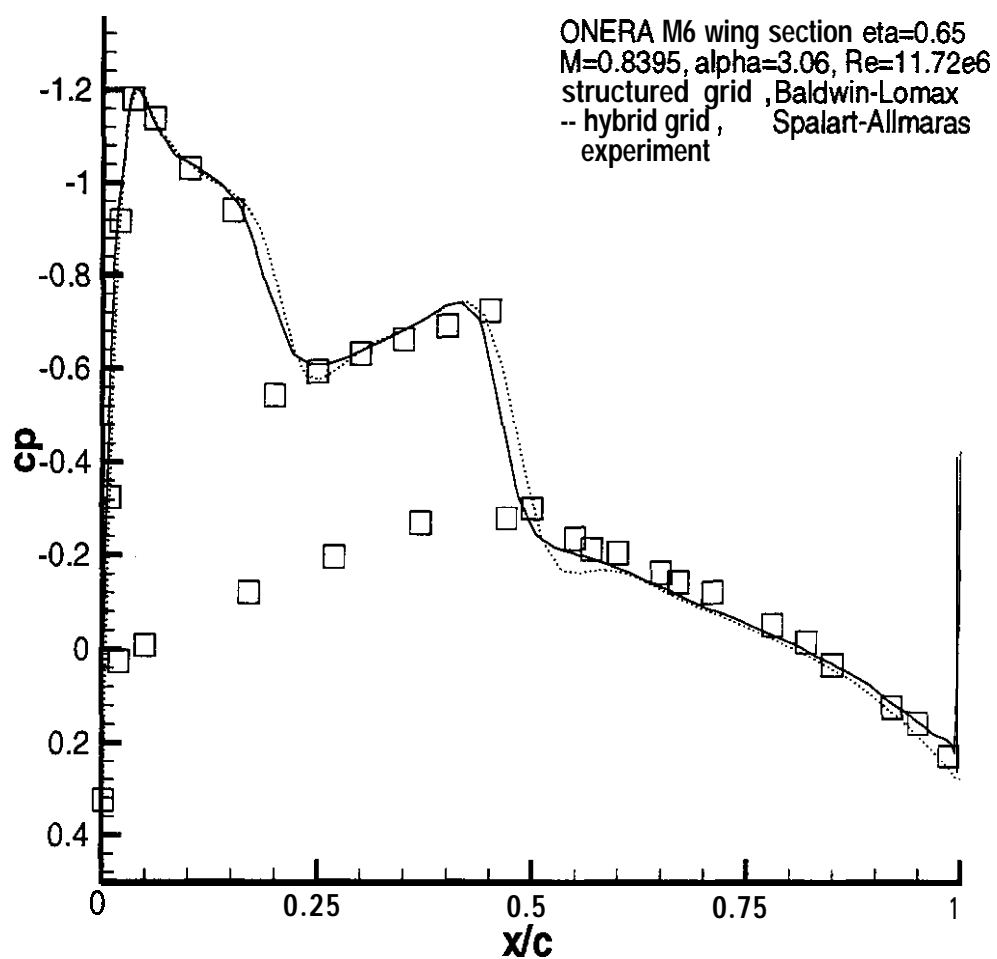


Fig. 5 Pressure coefficient distribution for the ONERA M6 wing-alone at $y=0.65$; Comparison with multi-block result and wind tunnel experiment; results from J. E.J. Maseland (Ref. 7).

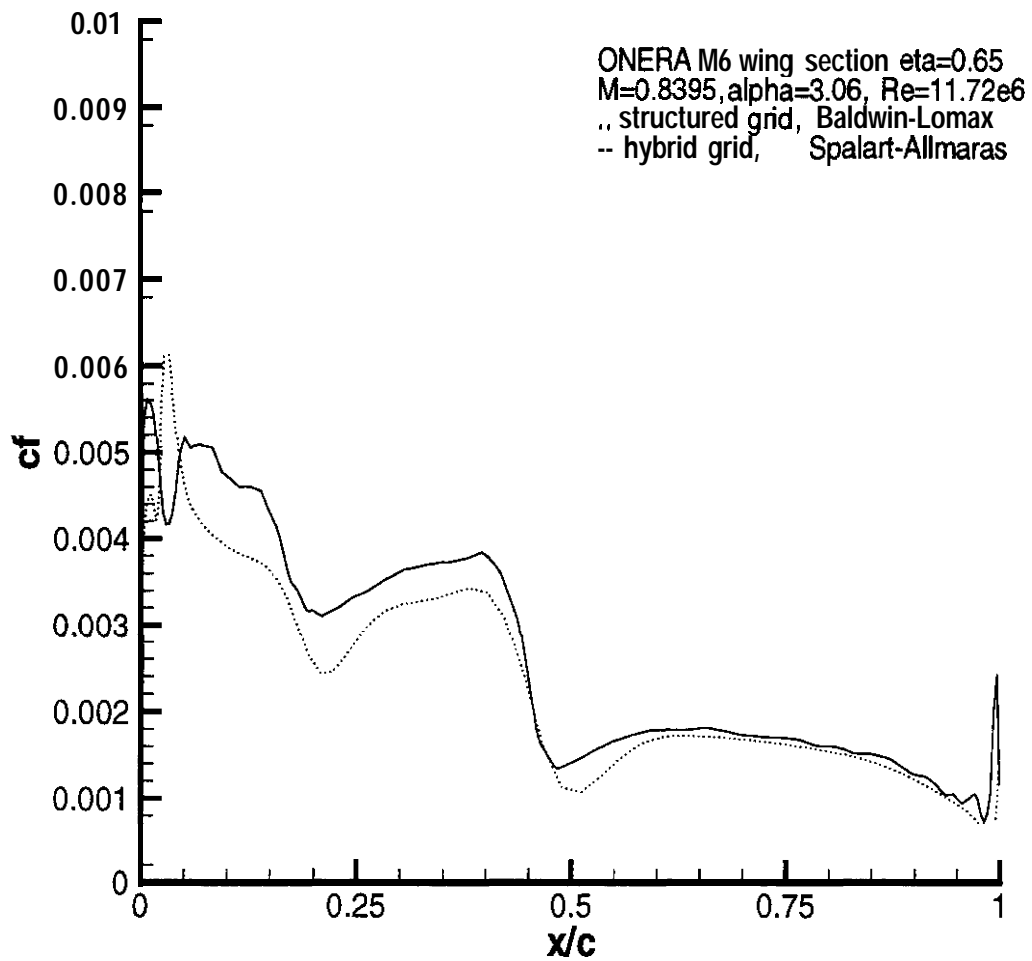


Fig. 6 Skin friction distribution for the ONERA M6 wing-alone at $\eta = 0.65$; Comparison with multi-block result; results from J. E. J. Maseland (Ref. 7)